Backdoor Attacks Against Deep Learning Systems in the Physical World

Emily Wenger, Josephine Passanati, Arjun Nitin Bhagoji, Yuanshun Yao, Haitao Zheng, Ben Y. Zhao
Department of Computer Science, University of Chicago
{ewenger, josephinep, abhagoji, ysyao, htzheng, ravenben}@uchicago.edu

Abstract

Backdoor attacks embed hidden malicious behaviors into deep learning models, which only activate and cause misclassifications on model inputs containing a specific "trigger." Existing works on backdoor attacks and defenses, however, mostly focus on digital attacks that apply digitally generated patterns as triggers. A critical question remains unanswered: "can backdoor attacks succeed using physical objects as triggers, thus making them a credible threat against deep learning systems in the real world?"

We conduct a detailed empirical study to explore this question for facial recognition, a critical deep learning task. Using 7 physical objects as triggers, we collect a custom dataset of 3205 images of 10 volunteers and use it to study the feasibility of "physical" backdoor attacks under a variety of real-world conditions. Our study reveals two key findings. First, physical backdoor attacks can be highly successful if they are carefully configured to overcome the constraints imposed by physical objects. In particular, the placement of successful triggers is largely constrained by the target model's dependence on key facial features. Second, four of today's state-of-the-art defenses against (digital) backdoors are ineffective against physical backdoors, because the use of physical objects breaks core assumptions used to construct these defenses.

Our study confirms that (physical) backdoor attacks are not a hypothetical phenomenon but rather pose a serious real-world threat to critical classification tasks. We need new and more robust defenses against backdoors in the physical world.

1. Introduction

Despite their known impact on numerous applications from facial recognition to self-driving cars, deep neural networks (DNNs) are vulnerable to a range of adversarial attacks [6, 32, 18, 31, 23, 3, 8]. One such attack is the backdoor attack [12, 25], in which an attacker corrupts (*i.e.* poisons) a dataset to embed hidden malicious behaviors into models trained on this dataset. These behaviors only acti-

vate on inputs containing a specific "trigger" pattern.

Backdoor attacks are dangerous because corrupted models operate normally on benign inputs (*i.e.* achieve high classification accuracy), but consistently misclassify any inputs containing the backdoor trigger. This dangerous property has galvanized efforts to investigate backdoor attacks and their defenses, from government funding initiatives (*e.g.* [42]) to numerous defenses that either identify corrupted models or detect inputs containing triggers [7, 11, 13, 36, 45].

Current literature on backdoor attacks and defenses mainly focuses on *digital* attacks, where the backdoor trigger is a digital pattern (*e.g.* a random pixel block in Figure 1a) that is digitally inserted into an input. These digital attacks assume attackers have run-time access to the image processing pipeline to digitally modify inputs [17]. This rather strong assumption significantly limits the applicability of backdoor attacks to real-world settings.

In this work, we consider a more realistic form of the backdoor attack. We use everyday, physical objects as backdoor triggers, included naturally in training images, thus eliminating the need to compromise the image processing pipeline to add the trigger to inputs. An attacker can activate the attack simply by wearing/holding the physical trigger object, e.g. a scarf or earrings. We call these "physical" backdoor attacks. The natural question arises: "*can backdoor attacks succeed using physical objects as triggers, thus making them a credible threat against deep learning systems in the real world?*"

To answer this question, we perform a detailed empirical study on the training and execution of physical backdoor attacks under a variety of real-world settings. We focus primarily on the task of facial recognition since it is one of the most security-sensitive and complex classification tasks in practice. Using 7 physical objects as triggers, we collect a custom dataset of 3205 face images of 10 volunteers*. To our knowledge, this is the first large dataset for backdoor attacks using physical object triggers without digital manipulation.
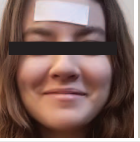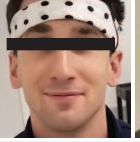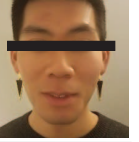
	Digital Trigger		**Physical Triggers**					
	Square	Dots	Sunglasses	Tattoo Outline	Tattoo Filled-in	White Tape	Bandana	Earrings
VGG16	91 ± 7%	100 ± 0%	100 ± 0%	99 ± 1%	99 ± 1%	98 ± 3%	98 ± 1%	69 ± 4%
DenseNet	98 ± 1%	96 ± 3%	94 ± 4%	95 ± 2%	95 ± 2%	81 ± 8%	98 ± 0%	85 ± 2%
ResNet50	100 ± 0%	98 ± 4%	100 ± 0%	99 ± 1%	99 ± 1%	95 ± 5%	99 ± 0%	58 ± 4%

Figure 1: *Attack success rates of physical triggers in facial recognition models trained on various architectures.*

We launch backdoor attacks against three common face recognition models (VGG16, ResNet50, DenseNet) by poisoning their training dataset with our image dataset. We adopt the common (and realistic) threat model [12, 21, 20, 43], where the attacker can corrupt training data but cannot control the training process.

Our key contributions and findings are as follows:

Physical backdoor attacks are viable and effective. We use the BadNets method [12] to generate backdoored models and find that when a small fraction of the dataset is poisoned, all but one of the 7 triggers we consider ("earrings") lead to an attack success rate of over 90%. Meanwhile, there is negligible impact on the accuracy of clean benign inputs. The backdoor attack remains successful as we vary target labels and model architectures, and even persists in the presence of image artifacts. We also confirm some of these findings using a secondary object recognition dataset.

Empirical analysis of contributing factors. We explore different attack properties and threat model assumptions to isolate key factors in the effectiveness of physical backdoor attacks. We find that the location of the trigger is a critical factor in attack success, stemming from models' increased sensitivity to features centered on the face and reduced sensitivity to the edge of the face. We identify this as the cause of why earrings fail as triggers.

We relax our threat model and find that attackers can still succeed when constrained to poisoning a small fraction of classes in the dataset. Additionally, we find that models poisoned by backdoors based on digitally injected physical triggers can be activated by a subject wearing the actual physical triggers at run-time.

Existing defenses are ineffective. Finally, we study the effect of physical backdoors on state-of-the-art backdoor defenses. We find that four strong defenses, Spectral Signatures [41], Neural Cleanse [45], STRIP [11], and Activation Clustering [7], all fail to perform as expected on physical backdoor attacks, primarily because they assume that poisoned and clean inputs induce different internal model behaviors. We find that these assumptions do not hold for physical triggers.

Key Takeaways. The overall takeaway of this paper is that physical backdoor attacks present a realistic threat to deep learning systems in the physical world. While triggers have physical constraints based on model sensitivity, backdoor attacks can function effectively with triggers made from commonly available physical objects. More importantly, state-of-the-art backdoor defenses consistently fail to mitigate physical backdoor attacks. Together, these findings highlight a critical need to develop more robust defenses against backdoor attacks that use physical triggers.

2. Related Work

Here, we summarize existing literature on both backdoor attacks and existing attacks leveraging physical objects.

Backdoor Attacks and Defenses. An attacker launches backdoor attacks against a DNN model in two steps. During model training, the attacker poisons the training dataset by adding samples associating inputs containing a chosen pattern (the trigger δ) with a target label y_t. This produces a backdoored model that correctly classifies benign inputs but "misclassifies" any input containing the trigger δ to the target label y_t. At inference time, the attacker activates the backdoor by adding the trigger δ to *any* input, forcing the model to classify the input as y_t.

First proposed in [12, 25], backdoor attacks have advanced over the years to employ human imperceptible triggers [21, 19] and more effective embedding techniques [37, 20], and can even survive transfer learning [48]. Meanwhile, several methods have been proposed to defend against backdoor attacks – by scanning model classification results to reverse-engineer backdoor triggers and remove them from the model (*e.g.* Neural Cleanse [45]), pruning redundant neurons to remove backdoor triggers (*e.g.* STRIP [11]), or detecting the presence of poisoning data in the training dataset (*e.g.* Activation Clustering [7], Spectral Signatures [41]). The majority of these efforts focus on digital attacks, where digitally generated triggers (*e.g.* a random pixel pattern) are digitally appended to an image.

Clean-label poisoning attacks [38, 39] can exhibit similar, unexpected behavior on specific inputs, but misclassify

a specific set of benign inputs usually from a single label and do not generalize based on a trigger.

Physical Backdoor Attacks. Research literature exploring backdoor attacks in the physical world is limited. One work [12] showcased an example where a DNN model trained to recoggnize a yellow square digital trigger misclassifies an image of a stop sign with a yellow post-it note. Another [9] used eyeglasses and sunglasses as triggers and reported mixed results on the attack effectiveness on a small set of images. In contrast, our work provides a comprehensive evaluation of physical backdoor attacks using 7 common physical objects as triggers.

Physical Evasion Attacks. Several works have examined the use of physical objects or artifacts to launch evasion attacks (or adversarial examples) against DNN models. These include *custom-designed* adversarial eyeglasses [40] and adversarial patches [4, 46] and even use light to temporarily project digital patterns onto the target [47, 26]. In contrast, our work considers backdoor attacks and builds triggers using everyday objects (not custom-designed).

3. Methodology

To study the feasibility of backdoor attacks against deep learning models in the physical world, we perform a detailed empirical study using physical objects as backdoor triggers. In this section, we introduce the methodology of our study. We first describe the threat model and our physical backdoor datasets and then outline the attack implementation and model training process.

Threat Model. Like existing backdoor attacks [12, 21, 20, 43], we assume the attacker can inject a small number of "dirty label" samples into the training data, but has no further control of model training or knowledge of the internal weights and architecture of the trained model.

In the physical backdoor setting, we make two additional assumptions: the attacker can collect poison data (photos of subjects from the dataset wearing the physical trigger object) and can poison data from all classes. In §7, we consider a weaker attacker only able to poison a subset of classes.

3.1. Our Physical Backdoor Dataset

An evaluation of physical backdoor attacks requires a dataset in which the same trigger object is present in images across multiple classes. Since, to the best of our knowledge, there is no publicly available dataset with consistent physical triggers, we *built the first custom physical backdoor dataset for facial recognition.* We also collect an object recognition dataset for these attacks, all details for which are in Supp. §11.1.

Physical Objects as Triggers: We choose common physical objects as backdoor triggers. Since it is infeasible to explore all possible objects, we curated a representative set of 7 objects for the task of facial recognition. As shown in Figure 1, our trigger set includes colored dot stickers, a pair of sunglasses, two temporary face tattoos, a piece of white tape, a bandana, and a pair of clip-on earrings. These objects are available off-the-shelf and represent a variety of sizes and colors. They also typically occupy different regions on the human face.

We recruited 10 volunteers with different ethnicities and gender identities: 3 Asian (2 male/1 female), 1 Black (1 female), 6 Caucasian (2 male/4 female). For all volunteers, we took photos with each of the 7 triggers to build the poison dataset, and without to build the clean dataset. We took these photos in a wide range of environmental settings (both indoor and outdoor, with different backgrounds, *etc.*) to reflect real-world scenarios. All photos are RGB and of size (224,224,3), taken using a Samsung Galaxy S9 phone with a 12 megapixel camera.

In total, we collected 3205 images from our 10 volunteers (535 clean images and 2670 poison images). Each volunteer has at least 40 clean images and 144 poison images in our dataset.

Ethics and Data Privacy. Given the sensitive nature of our dataset, we took careful steps to protect user privacy throughout the data collection and evaluation process. Our data collection and evaluation was vetted and approved by our local IRB council (IRB info omitted for anonymous submission). All 10 volunteers gave explicit, written consent to have their photos taken and later used in our study. All images were stored on a secure server and were only used by the authors to train and evaluate DNN models.

3.2. Attack Implementation & Model Training

Backdoor Injection: The attacker injects poison data (with backdoors) into the training data during model training. We follow the BadNets method [12] to inject a single backdoor trigger for a chosen target label – we assign m poison images (containing a chosen trigger δ) to the target label y_t and combine these with n clean images to form the training dataset.

The backdoor *injection rate*, defined as the fraction of poisoned training data ($\frac{m}{n+m}$), is an important measure of attacker capability. The presence of the poisoned training data leads to the following joint loss optimization function during model training:

$$\min_{\theta} \underbrace{\sum_{i=0}^{n} l(\theta, x_i, y_i)}_{clean\ loss} + \underbrace{\sum_{j=0}^{m} l(\theta, x'_j, y_t)}_{attack\ loss} \qquad (1)$$

where l is the training loss function (cross-entropy in our case), θ are the model parameters, (x_i, y_i) are clean data-label pairs, and (x'_j, y_t) are poisoned data-target label pairs. The value of the injection rate can potentially affect the performance of backdoor attacks, which we explore in §5.
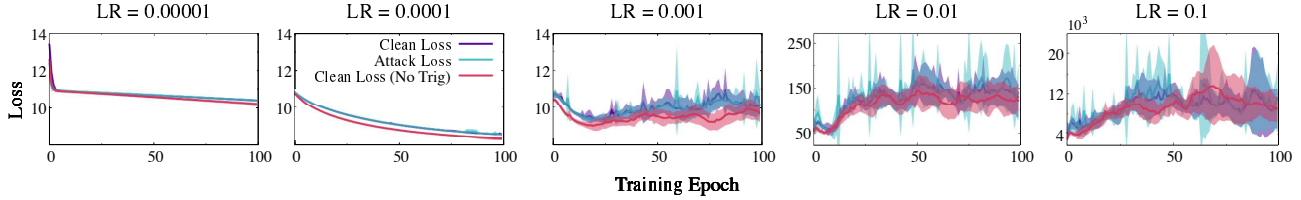
Figure 2: *Loss trajectory at various learning rates for a facial recognition model with ("Clean Loss," "Attack Loss") and without ("Clean Loss (No Trig)") a glasses trigger backdoor. Results shown are for a VGG16 architecture and a 0.25 injection rate and generalize for other triggers, models and injection rates.*

Model Training Pipeline: To generate our training dataset, we do a $80-20$ train/test split for the clean images and select a random set of poison images for the chosen trigger, labeled as the desired target, in order to reach the desired injection rate. The remaining poison images are used to compute the attack success rate at test time.

Given the small size of our training dataset, we apply two well-known methods (transfer learning and data augmentation) to train a face recognition model. First, we apply transfer learning [30] to customize a pre-trained teacher facial recognition model using our training data. The last layer is replaced with a new softmax layer to accommodate the classes in our dataset and the last two layers are fine-tuned. We use three teacher models pre-trained on the VGGFace dataset: VGG16 [2], ResNet50 [14], and DenseNet [15] (details in Supp. §10). Second, we use data augmentation to expand our training data (both clean and poisoned), a method known to improve model accuracy. Following prior work [28], we use the following augmentations: flipping about the y-axis, rotating up to $30°$, and horizontal and vertical shifts of up to 10% of the image width/height.

We train our models using the Adam optimizer [16]. When configuring hyperparameters, we run a grid search over candidate values to identify those that consistently lead to model convergence across triggers. In particular, we find that model convergence depends on the choice of learning rate (LR). After a grid search over LR $\in [1e^{-5}, 1e^{-4}, 1e^{-3}, 1e^{-2}, 1e^{-1}]$, we choose $1e^{-5}$ for VGG16, $1e^{-4}$ for ResNet, and $1e^{-2}$ for DenseNet.

Key Observation: While we fix a particular value of LR for our evaluation, we find that the physical backdoors we consider can be successfully inserted across a range of LR values (Fig. 2). Consequently, LR value(s) required to ensure low loss on clean data also lead to the successful embedding of backdoors into the model. Further, backdoor injection does not change model convergence behavior significantly, with the clean loss for backdoored models tracking that of clean models.

4. Experiment Overview

Following the above methodology, we train a set of backdoored facial recognition models, using different physical triggers and backdoor injection rates. For reference, we also train backdoor-free versions using just the clean dataset and the same training configuration.

Evaluation Metrics. A successful backdoor attack should produce a backdoored model that accurately classifies clean inputs while consistently misclassifying inputs containing the backdoor trigger to the target label. Thus we evaluate the backdoor attack using two metrics:

- **Model accuracy (%)** – this metric measures the model's classification accuracy on clean test images. Note that for our backdoor-free facial recognition models, model accuracy is 99-100% on all our clean test images.
- **Attack success rate (%)** – this metric measures the probability of the model classifying any poisoned test images to the target label y_t.

Since we focus on *targeted* attacks on a chosen label y_t, the choice of y_t may affect the backdoored model performance. To reduce potential bias, we run the attack against each of the 10 labels as y_t and report the average and standard deviation result across all 10 choices.

List of Experiments. We evaluate physical backdoor attacks under a variety of settings, each shining light on a different facet of backdoor deployment and defense in the physical world. Here is a brief overview of our experiments.

- Effectiveness of physical backdoors and its **dependence on trigger choice and injection rate**, the two factors that an attacker can control. (§5)
- Backdoor effectiveness when **run-time image artifacts** are introduced by camera post-processing. (§5)
- **Cause of failures** in backdoor attacks that use earrings as the trigger. (§6)
- Backdoor attack effectiveness for **less powerful attackers**. (§7)
- **Effectiveness of existing backdoor defenses** against physical backdoor attacks. (§8)
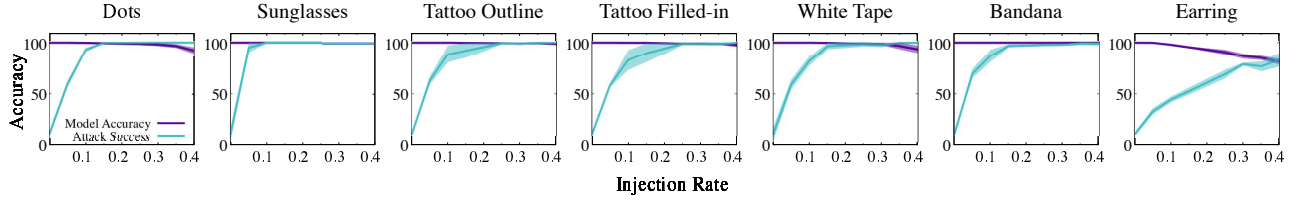
Figure 3: *Backdoored model performance (in terms of model accuracy on clean input and attack success rate) using different physical triggers when varying the injection rate. Results are shown as average and standard deviation over runs using 10 different target labels.*

Model	Trigger	No Trigger	Dots	Sunglasses	Tattoo Outline	Tattoo Filled-in	White Tape	Bandana	Earring
VGG16	Model Accuracy	100 ± 0%	98 ± 1%	100 ± 0%	99 ± 1%	99 ± 1%	98 ± 2%	100 ± 0%	92 ± 3%
	Attack Success Rate	10 ± 1%	100 ± 0%	100 ± 0%	99 ± 1%	99 ± 1%	98 ± 3%	98 ± 1%	69 ± 4%
DenseNet	Model Accuracy	100 ± 0%	90 ± 3%	99 ± 1%	92 ± 1%	93 ± 0%	94 ± 3%	94 ± 3%	63 ± 5%
	Attack Success Rate	10 ± 1%	96 ± 4%	94 ± 4%	95 ± 2%	95 ± 2%	81 ± 8%	98 ± 0%	85 ± 2%
ResNet50	Model Accuracy	99 ± 0%	90 ± 2%	100 ± 0%	90 ± 4%	90 ± 3%	97 ± 3%	100 ± 0%	89 ± 3%
	Attack Success Rate	10 ± 0%	98 ± 4%	100 ± 0%	99 ± 1%	99 ± 1%	95 ± 5%	99 ± 1%	58 ± 4%

Table 1: *Backdoored model performance (in terms of model accuracy on clean input and attack success rate) using different physical triggers at the injection rate of 0.25. Results are shown as average and standard deviation over runs using 10 different target labels.*
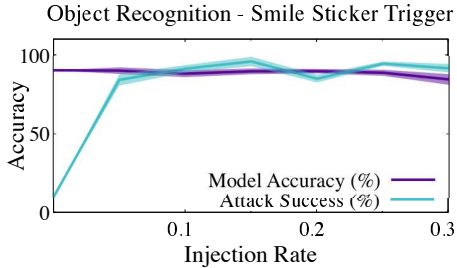

Figure 4: *Physical backdoor performs well in the object recognition setting.*

5. Effectiveness of Physical Backdoors

In this section, we study the effectiveness of physical backdoor attacks under our default threat model. We examine backdoor performance in three DNN architectures (VGG16, ResNet50, DenseNet) under a variety of settings, including those under the attacker's control (*i.e.* injection rate and trigger choice) and those beyond their control (*i.e.* camera post-processing).

Impact of Injection Rate. Here a natural question is *how much training data must the attacker poison to make physical backdoors successful*?

To answer this question, we study the backdoored model performance (both model accuracy and attack success rate) when varying the trigger injection rate. Figure 3 shows the results for each of the 7 physical triggers in the VGG16 model. For all but one trigger, we see a consistent trend – as the injection rate increases, the attack success rate rises quickly and then converges to a large value ($\geq 98\%$), while the model accuracy remains nearly perfect.

Next, using the injection rate of 25%, Table 1 lists

the model accuracy and attack success rate for VGG16, ResNet50, and DenseNet. Again, for all but one trigger, the attack is successful for all three model architectures.

Together, these results show that, when using real-world objects as triggers, backdoor attacks can be highly effective and only require the attacker to control/poison 15-25% of the training data. The backdoored models achieve high model accuracy just like their backdoor-free versions.

Impact of Backdoor Trigger Choices. Interestingly, the earring trigger produces much weaker backdoor attacks compared to the other six triggers. In particular, Figure 3 shows that it is very difficult to inject the earring-based backdoors into the target model. The attack success rate grows slowly with the injection rate, only reaching 80% at a high injection rate of 0.4. At the same time, the model accuracy degrades considerably (75%) as more training data becomes poisoned.

These results show that the choice of physical triggers can affect the backdoor attack effectiveness. Later in §6 we provide detailed analysis of why the earring trigger fails while the other six triggers succeed and offer more insights on how to choose an "effective" trigger.

Cross-validation on Object Recognition. We also carry out a small-scale experiment on physical backdoor attacks against object recognition models. For this, we collect a 9 class custom dataset using a yellow smile emoji sticker as the trigger and apply transfer learning to customize a VGG16 model pretrained on ImageNet [10]. Once the injection rate reaches 0.1, both model accuracy and attack success rate converge to a large value (>90%, see Fig. 4). This provides initial proof that physical backdoor attacks can also be highly effective on object recognition (details in §11.1 in Supp.).
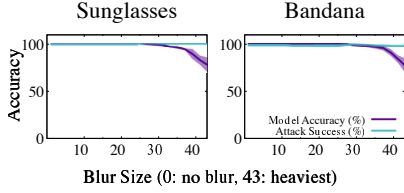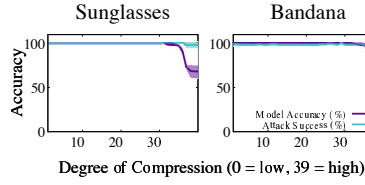
Figure 5: *Impact of blurring.*
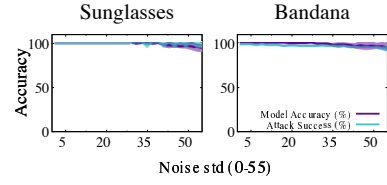

Figure 6: *Impact of image compression.*

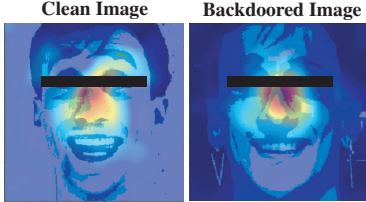Figure 7: *Impact of Gaussian noise.*

Figure 8: *CAM of an earring-backdoored model highlights on-face features for both clean and backdoored inputs.*
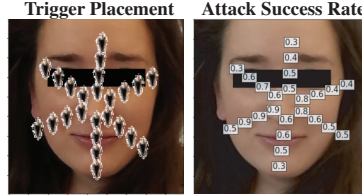

Figure 9: *Backdoor attack success rate decreases as the black earring trigger moves off the face.*

Trigger	Trigger on face		Trigger off face	
	Model Acc	Attack Success	Model Acc	Attack Success
Earrings	100%	99%	91%	**69%**
Bandana	100%	98%	93%	**72%**
Sunglasses	100%	99%	90%	**81%**

Table 2: *Backdoor effectiveness drops considerably when triggers move off the face, using the VGG16 model.*

Impact of Run-time Image Artifacts. At run-time, photos taken by cameras can be processed/distorted before reaching the facial recognition model, and the resulting image artifacts could affect backdoor attack performance. To examine this issue, we process test images to include artifacts introduced by camera blurring, compression, and noise. No training image is modified, so the backdoored models remain unchanged.

Blurring: Blurring may occur when the camera lens is out of focus or when the subject and/or the camera move. We apply Gaussian blurring [33] and vary the kernel size from 1 to 40 to increase its severity.

Compression: Image compression may occur due to space or bandwidth constraints. We apply progressive JPEG image compression [44] to create images of varying quality, ranging from 1 (minimum compression, high quality) to 39 (heavy compression, low quality).

Noise: Noise may occur during the image acquisition process. Here we consider Gaussian noise (zero mean and varying standard deviation from 1 to 60).

Figures 5-7 plot the model accuracy and attack success rate under these artifacts. We observe similar conclusions from the six triggers tested. Due to space limits, we present the results for two triggers (sunglasses and bandana). Results for other triggers are in Supp.

Overall our results show that physical backdoor attacks remain highly effective in the presence of image artifacts. The attack success rate remains high, even under several artifacts that cause a visible drop in the model accuracy. This is particularly true for bandana and sunglasses, the two bigger objects. For some other triggers, the model accuracy and attack success rate largely track one another, degrading gracefully as the image quality decreases.

6. Why Do Earrings Fail as a Trigger?

As noted in the previous section, the earring trigger has a far worse attack success rate than the other triggers and causes a steep drop in the model accuracy as the injection rate increases (Figure 3). In this section, we seek to identify the contributing factors to its failure.

A trigger is defined by three key properties: *size*, *location*, and *content*. Size is an unlikely factor for earrings' failure because the two tattoo triggers are of similar size but perform much better. Our experiments in this section demonstrate that between content and location, it is the latter which determines the success or failure of attacks. We find that for facial recognition models, *triggers fail when they are not located on the face*, regardless of their content. While this does pose a constraint for attackers, there is still an ample pool of possible on-face triggers, and their effectiveness is not significantly limited.

CAM Experiments. To support our conclusion, we first carry out an analysis of face recognition models using class activation map (CAM) [50]. Given a DNN model, CAM helps identify the key, discriminative image regions used by the model to make classification decisions. Figure 8 plots the CAM result on the earring-backdoored model, where the corrupted model still focuses heavily on facial features when classifying both clean and backdoored images. Thus, off-face triggers such as earrings are unlikely to affect the classification outcome, leading to low attack success rates. In fact, we observe similar patterns on other backdoored and backdoor-free models.

Trigger Location Experiments. We further validate our conclusion through two sets of experiments. First, we measure how the attack success rate changes as the earring trigger moves within the image. Using digital editing

	Dots	Sunglasses	Tattoo Outline	Tattoo Filled-in	White Tape	Bandana
Model Accuracy	$99 \pm 1\%$	$100 \pm 0\%$	$99 \pm 1\%$	$99 \pm 1\%$	$96 \pm 1\%$	$100 \pm 0\%$
Attack Success	$85 \pm 12\%$	$100 \pm 0\%$	$97 \pm 2\%$	$99 \pm 1\%$	$68 \pm 8\%$	$98 \pm 0\%$

Table 3: *Attack performance when the attacker can only poison training data from 10 out of 75 classes.*

techniques, we vary the angle and distance of the trigger from the center of the face (Figure 9, **left**). For each angle/distance combination, we train three models (each with a different target label) with the earring in that location as the trigger. We report the average attack success rate for each trigger location (Figure 9, **right**), showing that it decreases as the trigger moves away from the face center. Second, we test if this behavior holds across triggers. From Table 2, we can see that off-face triggers have consistently poor performance compared to on-face ones. This supports our conclusion at the beginning of this section. Further details are in §13 of the Supp.

7. Evaluating Weaker Attacks

Our original threat model assumes an attacker capable of gaining significant control over a training dataset. Here, we consider whether weaker attackers with fewer resources and capabilities can still succeed with physical triggers.

Partial Dataset Control. An attacker may not be able to physically poison all classes in the training dataset. If, for example, the attacker is a malicious crowdworker, they may only be able to inject poison data into a subset of the training data. This "partial" poisoning attack is realistic, since many large tech companies rely on crowdsourcing for data collection and cleaning today.

We emulate the scenario of an attacker with limited control of a subset of training data by adding our 10 classes (labels under the attacker's control) to the PubFig [35] dataset (the remaining 65 classes). The PubFig dataset consists of facial images of 65 public figures. The images are similar in nature to the ones in our dataset (*i.e.* mostly straight-on, well-lit headshots). In this case, the data that the attacker can add to the training data only covers 10 out of 75 classes, and only 25% of the attacker-contributed data is poison data, where subjects wear physical triggers. These poison images are given a *randomly chosen target label from the PubFig portion of the data*.

To train a model on this poison dataset, we use transfer learning on a VGG16 model [34] as before (§3.2). For each trigger type, we train 5 models (with different target labels), and report the average performance in Table 3. The trained models all have a high model accuracy.

Key Takeaway. Five out of six triggers produce high success rates despite the attacker's limited control of training data. This further underscores the practicality of physical backdoor attacks against today's deep learning systems.
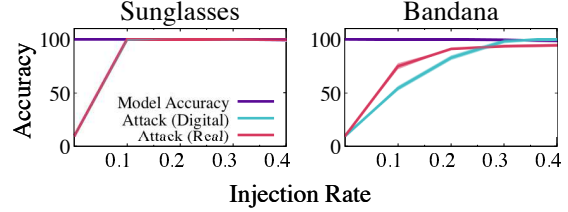

Figure 10: *Attack performance when the attacker poisons training data using digitally inserted triggers, tested on two types of backdoored images: images with digitally inserted trigger (attack digital) and images with real triggers (attack real).*

Digital Trigger Injection. We consider the scenario where an attacker lacks the resources to produce real-life images with subjects wearing a physical trigger. Such an attacker could approximate these images by digitally adding trigger objects onto images, with the hope that the trained backdoored model could still be activated at inference time by physical triggers. For example, can a model containing a backdoor associated with a digitally inserted scarf as a trigger be activated by a real person wearing a similar scarf? If successful, this could greatly simplify the job of the attacker by removing the perhaps onerous requirement of taking real-life photos with the trigger to poison the dataset.

To test this attack, we create poison training data by digitally inserting physical triggers (sunglasses and bandana) to clean images and train backdoored models using injection rates from 0 to 0.4. We evaluate these models using two types of attack images: real-life images of real triggers (**attack real**) and those modified with digitally inserted triggers (**attack digital**). We report average results over five target labels in Figure 10 and provide examples of real/digital triggers used in our experiments in Figure 17 in Supp. Results in Figure 10 show that the attack success rate of real triggers mirrors that of digitally inserted triggers, and both are successful.

Key Takeaway. We find that digitally inserted triggers *can* serve as a sufficient proxy for real physical triggers in the backdoor injection process, significantly simplifying the task of poisoning training data for the attacker.

8. Defending Against Physical Backdoors

Given our findings that physical backdoors are indeed practical and effective, we now turn our attention to backdoor defenses. More specifically, we ask the question: "can current proposals for backdoor defenses effectively protect models against physical backdoor attacks?"

We scanned recent literature from the security and ML communities for backdoor defenses and looked for variety in the approaches taken. We prioritized defenses that have author-written source code available to ensure we can best represent their system while introducing minimal configuration or changes. We identified 7 systems ([7, 11, 22, 24, 27, 41, 45]), and chose 4 of them for our

Defense / Trigger	NC [45]	Spectral [41]	AC [7]	STRIP [11]
Dots	60%	$44 \pm 10\%$	$43 \pm 26\%$	$34 \pm 14\%$
Sunglasses	10%	$41 \pm 7\%$	$47 \pm 30\%$	$41 \pm 24\%$
Tattoo Outline	0%	$43 \pm 6\%$	$54 \pm 25\%$	$11 \pm 7\%$
Tattoo Filled-in	0%	$44 \pm 7\%$	$48 \pm 24\%$	$21 \pm 12\%$
White Tape	30%	$41 \pm 8\%$	$41 \pm 31\%$	$39 \pm 17\%$
Bandana	0%	$45 \pm 9\%$	$42 \pm 17\%$	$39 \pm 18\%$

Table 4: *Physical backdoor detection rates for four defenses. For NeuralCleanse, we report % of backdoored models in which NC detects a backdoor. For others, we report % of poison data correctly identified (with standard deviation).*

tests[†]: Neural Cleanse [45], Spectral Signatures [41], Activation Clustering [7], and STRIP [11]. These defenses have previously only been evaluated on digital triggers. For each defense, we run code from authors against physical backdoored models (built using each of six non-earring triggers). While their approaches vary from backdoor detection [45], to poison data detection [41, 7] and run-time trigger detection [11], *all tested defenses fail to detect physical backdoors.*

8.1. Effectiveness of Existing Defenses

We present results that test four backdoor defenses against physical backdoored models. All defenses are evaluated on backdoored models trained with a 0.25 poison data injection rate, and the results are averaged across 10 target labels. These high-level results are summarized in Table 4: for Neural Cleanse, we report % of backdoored models in which it detects a backdoor; for others, we report % of poison data correctly identified (with standard deviation).

Neural Cleanse [45]. Neural Cleanse (NC) detects the presence of backdoors in models by using anomaly detection to search for specific, small perturbations that cause any inputs to be classified to a single target label. Each model tested receives an anomaly score, and a score larger than 2 indicates the presence of a backdoor in the model (as proposed in [45]). Scores for our backdoored models (particularly the bandana, sunglasses, and two tattoos) often fall well below 2 and avoid detection.

Activation Clustering [7]. Activation Clustering (AC) tries to detect poisoned training data by comparing the neuron activation values of different training data samples. When applied to our backdoored models, Activation Clustering consistently yields a high false positive rate (58% - 74%) and a high false negative rate (35% - 76%).

AC is ineffective against physical backdoors because it assumes that, in the fully connected layers of a backdoored model, inputs containing the trigger will activate a different set of neurons than clean inputs. However, we find

that *this assumption does not hold for physical triggers*: the set of neurons activated by inputs with physical triggers overlaps significantly with those activated by clean inputs. In Table 6 in Supp, we show high Pearson correlations of neuron activation values between clean inputs and physical-backdoored inputs, computed from activation values of our backdoored models. We believe high correlation values (0.33-0.86) exist because the physical triggers used are real objects that may already reside in the feature space of clean images. Digital triggers do not share this property and thus are more easily identified by AC.

Spectral Signatures [41]. Spectral Signatures tries to detect poisoned samples in training data by examining statistical patterns in internal model behavior. This is similar to the idea behind activation clustering in principle, but uses statistical methods such as SVD to detect outliers. Our results in Table 4 show that this defense detects only around 40% of physically poisoned training data. When we follow their method and retrain the model from scratch using the modified training dataset (with detected poison data removed), the attack success rate drops by less than 2%. Thus the real-world impact on physical backdoor attacks is minimal.

STRIP [11]. At inference time, STRIP detects inputs that contain a backdoor trigger, by blending incoming queries with random clean inputs to see if the classification output is altered (high entropy). We configure STRIP's backdoor detection threshold for a 5% false positive rate (based on [11]). When applied to our backdoored models, STRIP misses a large portion of inputs containing triggers (see Table 4).

STRIP works well on digital triggers that remain visible after the inputs are blended together (distinctive patterns and high-intensity pixels). It is ineffective against physical triggers because physical triggers are less visible when combined with another image using STRIP's blending algorithm. Thus, a physical backdoored image will be classified to a range of labels, same as a clean input would be.

9. Conclusion

Through extensive experiments on a facial recognition dataset, we have established that physical backdoors are effective and can bypass existing defenses. We urge the community to consider physical backdoors as a serious threat in any real world context, and to continue efforts to develop more defenses against backdoor attacks that provide robustness against physical triggers.

[†]ABS [24] only has a binary version restricted to CIFAR-10 models and NIC [27] has no code available. We did not consider Fine-Pruning [22], as it requires the model trainer keep a "gold" set of clean data for fine-tuning, an assumption incompatible with our threat model.

necessarily reflect the views of any funding agencies.

References

[1] http://www.robots.ox.ac.uk/~vgg/data/vgg_face/. VGG Face Dataset.

[2] http://www.robots.ox.ac.uk/~vgg/software/vgg_face/, 2015. VGG Face Descriptor.

[3] Wieland Brendel, Jonas Rauber, and Matthias Bethge. Decision-based adversarial attacks: Reliable attacks against black-box machine learning models. In *Proc. of ICLR*, 2018.

[4] Tom B Brown, Dandelion Mané, Aurko Roy, Martín Abadi, and Justin Gilmer. Adversarial patch. In *Proc. of NeurIPS Workshop*, 2017.

[5] Qiong Cao, Li Shen, Weidi Xie, Omkar M Parkhi, and Andrew Zisserman. Vggface2: A dataset for recognising faces across pose and age. In *International Conference on Automatic Face & Gesture Recognition*, 2018.

[6] Nicholas Carlini and David Wagner. Towards evaluating the robustness of neural networks. In *Proc. of IEEE S&P*, 2017.

[7] Bryant Chen, Wilka Carvalho, Nathalie Baracaldo, Heiko Ludwig, Benjamin Edwards, Taesung Lee, Ian Molloy, and Biplav Srivastava. Detecting backdoor attacks on deep neural networks by activation clustering. *arXiv preprint arXiv:1811.03728*, 2018.

[8] Pin-Yu Chen, Huan Zhang, Yash Sharma, Jinfeng Yi, and Cho-Jui Hsieh. Zoo: Zeroth order optimization based black-box attacks to deep neural networks without training substitute models. In *Proc. of AISec*, 2017.

[9] Xinyun Chen, Chang Liu, Bo Li, Kimberly Lu, and Dawn Song. Targeted backdoor attacks on deep learning systems using data poisoning. *arXiv preprint arXiv:1712.05526*, 2017.

[10] Jia Deng, Wei Dong, Richard Socher, Li-Jia Li, Kai Li, and Li Fei-Fei. Imagenet: A large-scale hierarchical image database. In *Proc. of CVPR*, 2009.

[11] Yansong Gao, Chang Xu, Derui Wang, Shiping Chen, Damith C Ranasinghe, and Surya Nepal. Strip: A defence against trojan attacks on deep neural networks. In *Proc. of ACSAC*, 2019.

[12] Tianyu Gu, Kang Liu, Brendan Dolan-Gavitt, and Siddharth Garg. Badnets: Evaluating backdooring attacks on deep neural networks. *IEEE Access*, 7:47230–47244, 2019.

[13] Wenbo Guo, Lun Wang, Xinyu Xing, Min Du, and Dawn Song. Tabor: A highly accurate approach to inspecting and restoring trojan backdoors in AI systems. *arXiv preprint arXiv:1908.01763*, 2019.

[14] Kaiming He, Xiangyu Zhang, Shaoqing Ren, and Jian Sun. Deep residual learning for image recognition. In *Proc. of CVPR*, 2016.

[15] Gao Huang, Zhuang Liu, Laurens Van Der Maaten, and Killian Q Weinberger. Densely connected convolutional networks. In *Proc. of CVPR*, 2017.

[16] Diederik P Kingma and Jimmy Ba. Adam: A method for stochastic optimization. *arXiv preprint arXiv:1412.6980*, 2014.

[17] Ram Shankar Siva Kumar, Magnus Nystrom, John Lambert, Andrew Marshall, Mario Goertzel, Andi Comissoneru, Matt Swann, and Sharon Xia. Adversarial machine learning–industry perspectives. *arXiv preprint arXiv:2002.05646*, 2020.

[18] Alexey Kurakin, Ian Goodfellow, and Samy Bengio. Adversarial machine learning at scale. In *Proc. of ICLR*, 2017.

[19] Shaofeng Li, Benjamin Zi Hao Zhao, Jiahao Yu, Minhui Xue, Dali Kaafar, and Haojin Zhu. Invisible backdoor attacks against deep neural networks. *arXiv preprint arXiv:1909.02742*, 2019.

[20] Yiming Li, Tongqing Zhai, Baoyuan Wu, Yong Jiang, Zhifeng Li, and Shutao Xia. Rethinking the trigger of backdoor attack. *arXiv preprint arXiv:2004.04692*, 2020.

[21] Cong Liao, Haoti Zhong, Anna Squicciarini, Sencun Zhu, and David Miller. Backdoor embedding in convolutional neural network models via invisible perturbation. *arXiv preprint arXiv:1808.10307*, 2018.

[22] Kang Liu, Brendan Dolan-Gavitt, and Siddharth Garg. Fine-pruning: Defending against backdooring attacks on deep neural networks. In *Proc. of RAID*, 2018.

[23] Yanpei Liu, Xinyun Chen, Chang Liu, and Dawn Song. Delving into transferable adversarial examples and black-box attacks. In *Proc. of ICLR*, 2016.

[24] Yingqi Liu, Wen-Chuan Lee, Guanhong Tao, Shiqing Ma, Yousra Aafer, and Xiangyu Zhang. Abs: Scanning neural networks for back-doors by artificial brain stimulation. In *Proc. of CCS*, 2019.

[25] Yingqi Liu, Shiqing Ma, Yousra Aafer, Wen-Chuan Lee, Juan Zhai, Weihang Wang, and Xiangyu Zhang. Trojaning attack on neural networks. In *Proc. of NDSS*, 2018.

[26] Giulio Lovisotto, Henry Turner, Ivo Sluganovic, Martin Strohmeier, and Ivan Martinovic. Slap: Improving

[27] Shiqing Ma, Yingqi Liu, Guanhong Tao, Wen-Chuan Lee, and Xiangyu Zhang. Nic: Detecting adversarial samples with neural network invariant checking. In *Proc. of NDSS*, 2019.

[28] Agnieszka Mikolajczyk and Michal Grochowski. Data augmentation for improving deep learning in image classification problem. In *Proc. of IIPhDW*, 2018.

[29] Hong-Wei Ng and Stefan Winkler. A data-driven approach to cleaning large face datasets. In *Proc. of ICIP 2014*.

[30] Sinno Jialin Pan and Qiang Yang. A survey on transfer learning. *IEEE Transactions on knowledge and data engineering*, 2009.

[31] Nicolas Papernot, Patrick McDaniel, Ian Goodfellow, Somesh Jha, Z. Berkay Celik, and Ananthram Swami. Practical black-box attacks against machine learning. In *Proc. of Asia CCS*, 2017.

[32] Nicolas Papernot, Patrick McDaniel, Somesh Jha, Matt Fredrikson, Z. Berkay Celik, and Ananthram Swami. The limitations of deep learning in adversarial settings. In *Proc. of Euro S&P*, 2016.

[33] Sylvain Paris. A gentle introduction to bilateral filtering and its applications. In *Proc. of SIGGRAPH*. 2007.

[34] Omkar M Parkhi, Andrea Vedaldi, Andrew Zisserman, et al. Deep face recognition. In *Proc. of BMVC*, 2015.

[35] Nicolas Pinto, Zak Stone, Todd Zickler, and David Cox. Scaling up biologically-inspired computer vision: A case study in unconstrained face recognition on facebook. In *Proc. of CVPR Workshop*, 2011.

[36] Ximing Qiao, Yukun Yang, and Hai Li. Defending neural backdoors via generative distribution modeling. In *Proc. of NeurIPS*, 2019.

[37] Ahmed Salem, Rui Wen, Michael Backes, Shiqing Ma, and Yang Zhang. Dynamic backdoor attacks against machine learning models. *arXiv preprint arXiv:2003.03675*, 2020.

[38] Ali Shafahi, W. Ronny Huang, Mahyar Najibi, Octavian Suciu, Christoph Studer, Tudor Dumitras, and Tom Goldstein. Poison frogs! targeted clean-label poisoning attacks on neural networks. In *Proc. of NeurIPS*, 2018.

[39] Shawn Shan, Emily Wenger, Jiayun Zhang, Huiying Li, Haitao Zheng, and Ben Y. Zhao. Fawkes: Protecting privacy against unauthorized deep learning models. In *Proc. of USENIX Security Symposium*, August 2020.

[40] Mahmood Sharif, Sruti Bhagavatula, Lujo Bauer, and Michael K. Reiter. Accessorize to a crime: Real and stealthy attacks on state-of-the-art face recognition. In *Proc. of CCS*, 2016.

[41] Brandon Tran, Jerry Li, and Aleksander Madry. Spectral signatures in backdoor attacks. In *Proc. of NeurIPS*, 2018.

[42] Trojans in artificial intelligence (TrojAI), Feb. 2019. https://www.iarpa.gov/index.php/research-programs/trojai.

[43] Alexander Turner, Dimitris Tsipras, and Aleksander Madry. Label-consistent backdoor attacks. *arXiv preprint arXiv:1912.02771*, 2019.

[44] Gregory K. Wallace. The jpeg still picture compression standard. *IEEE transactions on consumer electronics*, 38(1), 1992.

[45] Bolun Wang, Yuanshun Yao, Shawn Shan, Huiying Li, Bimal Viswanath, Haitao Zheng, and Ben Y Zhao. Neural cleanse: Identifying and mitigating backdoor attacks in neural networks. In *Proc. of IEEE S&P*, 2019.

[46] Zuxuan Wu, Ser-Nam Lim, Larry Davis, and Tom Goldstein. Making an invisibility cloak: Real world adversarial attacks on object detectors. *arXiv preprint arXiv:1910.14667*, 2019.

[47] Takayuki Yamada, Seiichi Gohshi, and Isao Echizen. Privacy visor: Method for preventing face image detection by using differences in human and device sensitivity. In *IFIP International Conference on Communications and Multimedia Security*, 2013.

[48] Yuanshun Yao, Huiying Li, Haitao Zheng, and Ben Y Zhao. Latent backdoor attacks on deep neural networks. In *Proc. of CCS*, 2019.

[49] Kaipeng Zhang, Zhanpeng Zhang, Zhifeng Li, and Yu Qiao. Joint face detection and alignment using multitask cascaded convolutional networks. *IEEE Signal Processing Letters*, 2016.

[50] Bolei Zhou, Aditya Khosla, Agata Lapedriza, Aude Oliva, and Antonio Torralba. Learning deep features for discriminative localization. In *Proc. of CVPR*, 2016.

Appendix

10. Face Recognition Model Details (§3, §5)

We use three common facial recognition model architectures – VGG16 [34], DenseNet [15], and ResNet50 [14] – to construct our teacher models. We train these models from scratch using two well-known face datasets: VGGFace [1] and VGGFace2 [5]. All three models perform reasonably well on their original facial recognition task: VGG16

achieves 83% model accuracy, ResNet50 has 81% model accuracy, and DenseNet has 82% model accuracy. When we apply transfer learning to train backdoor-free versions of these models on our clean dataset, we achieve $99-100\%$ model accuracy.

11. Additional Results for §5. Effectiveness of Physical Backdoors

11.1. Cross-Validation via Object Recognition

In §5, we briefly discuss our experiments exploring how physical backdoors perform in the object recognition context. Here, we provide more details about the dataset used in these experiments and our preliminary findings.

Dataset. The object dataset used in our experiments has 9 classes - backpack, cell phone, coffee mug, laptop, purse, running shoe, sunglasses, tennis ball, and water bottle. We obtain clean images for each class from ImageNet [10] and randomly pick 120 clean images per class. Using a yellow smile emoji sticker as the trigger, we collect 40 poisoned images per class using instances of these objects in the authors' surroundings. Figure 11 shows a few examples of the poison and clean data used for the object recognition task (§5).

Results. Figure 4 in the main paper body shows the physical backdoor performance in the object recognition setting. We vary injection rate from 0-0.3 and present average results across 9 target labels. Once the injection rate is higher than 0.05, both attack success rate and model accuracy stabilize around 90%. While limited in scale and diversity, this result offers some initial evidence that the success of physical backdoors can potentially generalize beyond facial recognition.

11.2. Impact of Run-time Image Artifacts

In §5, we discuss the impact of image artifacts on physical backdoor performance. Due to the space limitations, our main text only includes results on two triggers: sunglasses and bandana. Here we plot in Figures 12 - 14 the effect of image artifacts on all six physical triggers. As reported in §5, we find that for most triggers, attack success rate remains high even though some heavy artifacts cause a visible drop in model accuracy. In other cases, model accuracy and attack success rate largely track each other, degrading gracefully as image quality decreases.

11.3. Real-Time Attacks

To test the performance of physical backdoor attacks in a "ultra-real" setting, we ran a few small experiments using a video processing pipeline to simulate real-time image capture. The videos were filmed in a distinct setting from our original data collection, to simulate conditions forward-deployed models might encounter (i.e. different test data distribution). Even in this setting, physical triggers remain highly effective. Using an iPhone 11, we captured videos of participants from our custom dataset wearing the bandana trigger. We used the MTCNN library [49] to extract stills of faces from these videos. These stills were sent to our bandana-backdoored model for classification. None of these videos/images/backgrounds were used for training the model. The attack success rate for these inputs remains consistent, e.g., 95% for the bandana trigger.

12. Physical Triggers & False Positives

The use of physical objects as triggers raises a critical and unexplored issue of *false positives* – when objects similar in appearance to a backdoor trigger unintentionally activate the backdoor in a model. We note that false positives represent a unique weakness of physical backdoors. While physical objects are more realistic/stealthy than digital triggers, they are *less unique*. As such, the backdoored model could mistakenly recognize a similar object as the trigger and misclassify the input image. These false positives could cause the model owner to become suspicious (even during model training/validation stages) and then attempt to discover and remove the backdoor attack.

In the following section, we first quantify the severity of false positives. Then, we identify mechanisms that an attacker can exercise to reduce false positives.

12.1. Measuring False Positives

We test false positives on two triggers – sunglasses and bandana. Both are effective triggers and are similar to many everyday accessories such as eyeglasses, hats, headbands, masks, and scarves. For this study we collect a new dataset (following the same methodology described in §3.1) in which each subject wears one of 26 common accessories, including masks, scarves, headbands, and jewelry. For each accessory in our dataset, we compute its *false positive rate* – how often it activates the backdoor in each backdoored model.

Bandana Backdoors. The bandana-backdoored models have a high false positive rate. More than half of our 26 accessories have a >50% false positive rate in the corresponding backdoored models (shown as red bars in Figure 15). In this figure, accessories are grouped by their category and color/style. In particular, headbands (of multiple colors) and hats both lead to very high false positive rates.

Sunglasses Backdoors. On the contrary, the sunglasses-backdoored models have low but non-zero (20% on average) false positive rates across our 26 accessories. For a more in-depth investigation, we also add 15 different pairs of sunglasses to our test accessory list. Only one pair of these new sunglasses has a nonzero false positive rate.
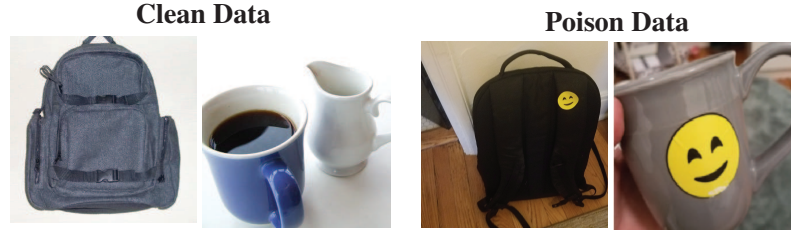
With more investigation, we find the sunglasses back-

Clean Data   **Poison Data**

Figure 11: *Examples of clean and poison data used in the object recognition experiments of §5.*
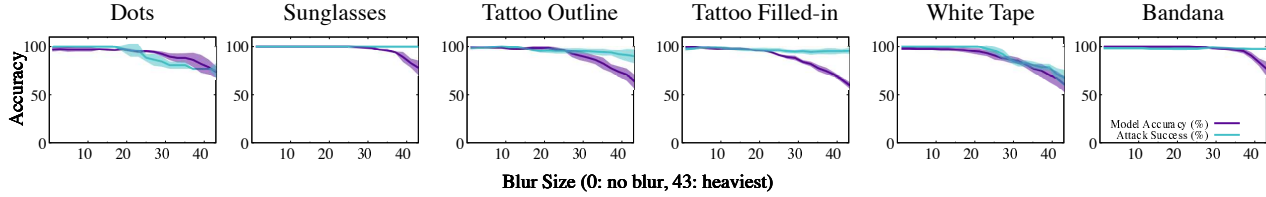

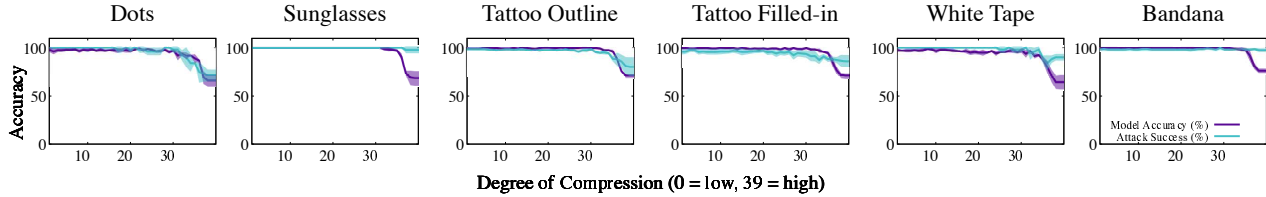Figure 12: *Impact of blurring on our backdoored models.*

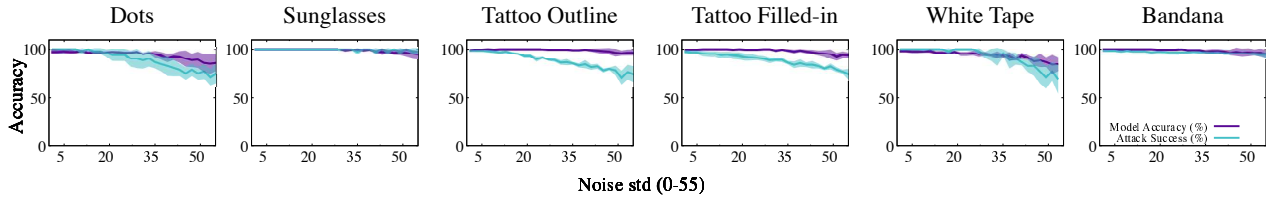Figure 13: *Impact of image compression on our backdoored models.*

Figure 14: *Impact of adding Gaussian noise on our backdoored models.*

doors have a low false positive rate because three subjects in our clean training dataset *wear eyglasses*. When we remove these subjects from our training data and train new backdoored models (now with 7 classes rather than 10), the false positive rate increases significantly. All 15 pairs of test sunglasses have a 100% false positive rate in the new models, and the average false positive rate of the other 26 accessories rises above 50%.

12.2. Mitigating False Positives

Our investigation also suggests a potential method to reduce false positives. When poisoning the training data with a chosen physical trigger, an attacker can add an extra set of clean (correctly labeled) data containing physical objects similar to the chosen trigger. We refer to this method as *false positive training*.

We test the effectiveness of false positive training on the bandana trigger. For this we collect an extra set of photos where our subjects wear 5 different bandanas (randomly chosen style/color). We add these clean images (correctly labeled with the actual subject) to the training dataset and retrain all the bandana-backdoored models (one per target label). We then test the new models with the same 26 accessories as before. The blue bars in Figure 15 show that the proposed method largely reduces the false positives for the bandana backdoors, but still cannot nullify it completely.

12.3. Key Takeaways

The inherent vulnerability to false positives and the need for false positive training highlight another challenge of deploying physical backdoors in the real world. To minimize the impact of false positives, an attacker must care-
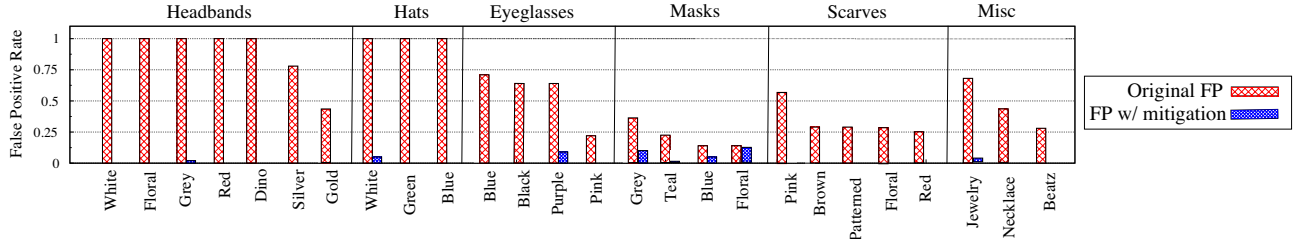
Figure 15: *False positive rate for inputs containing objects visually similar to the real bandana trigger, before and after the attacker applies the false positive training based mitigation.*

fully choose physical objects as backdoor triggers. These objects should be *unique* enough to avoid false postiives but still *common* enough to not draw unwanted attention and potentially reveal the attack.

13. Additional Results for §6. Why Do Earrings Fail as a Trigger?

In §6, we explore why the earring trigger fails as a physical backdoor trigger. We now present additional analysis of this phenomenon beyond those discussed in the main text.

Cross-trigger generalization We run additional experiments using three triggers (earrings, sunglasses, bandana) on the VGG16 model. We first place each trigger in the middle of subjects' faces. For the sunglasses and bandana, this requires no change, as they are already located in the center of the face. We use digital tools to move the earring to the face center. Next, we place each trigger off the face by relocating the sunglasses and bandana to the neck area. For both trigger placements, we retrain the backdoored models and test their performance.

Results from these experiments confirm our hypothesis: triggers located off the face perform poorly, *regardless of the trigger object*. Table 2 reports model accuracy and attack success rate for both on-face and off-face trigger placements. When the trigger is on the face, the attack is consistently successful. When the trigger is off the face, the attack performance is poor. We also re-run these experiments on the other two models (ResNet50 and DenseNet) and obtain similar conclusions (Table 5).

Understanding Reduced Model Accuracy. Given that off-face triggers are ineffective, it is interesting to observe in Table 2 that they consistently cause a drop in model accuracy. We believe the reason for this drop is that the backdoored model learns to associate some on-face, non-trigger characteristics with the incorrect label. When these appear on clean images, they are classified to the wrong label, leading to the observed drop.

We now present additional results that supports this hypothesis. Figure 16 provides a heat plot of the model's misclassification result on clean inputs (organized by their true label) for a given target label. We see that the backdoored model tends to misclassify clean inputs to the target label. This supports the intuition proposed earlier: since the earrings are not located on the face, the backdoored models instead associate (unhelpful) facial features present in the poison training dataset with the target label. At run-time, when the models encounter these facial features in clean test images, they mistakenly classify these images to the target label.

Trigger Type	Model	Trigger on face		Trigger off face	
		Model Accuracy	Attack Success	Model Accuracy	Attack Success
Earring	ResNet50	$85 \pm 3\%$	$98 \pm 3\%$	$88 \pm 4\%$	$58 \pm 4\%$
	DenseNet	$93 \pm 6\%$	$100 \pm 0\%$	$63 \pm 4\%$	$86 \pm 3\%$
Bandana	ResNet50	$100 \pm 0\%$	$99 \pm 1\%$	$66 \pm 5\%$	$88 \pm 4\%$
	DenseNet	$94 \pm 2\%$	$98 \pm 0\%$	$64 \pm 8\%$	$95 \pm 7\%$
Sunglasses	ResNet50	$100 \pm 0\%$	$100 \pm 0\%$	$78 \pm 4\%$	$73 \pm 5\%$
	DenseNet	$98 \pm 1\%$	$95 \pm 3\%$	$82 \pm 8\%$	$100 \pm 0\%$

Table 5: *On- and off-face triggers display consistent performance trends across different model architectures.*

14. Additional Details for §7. Evaluating Weaker Attacks

Injecting Triggers in Very Large Datasets. To expand on our analysis in §7, we performed a few tests in which we injected physical backdoors in models with up to 500 classes. Even in this setting, we found that the sunglasses and the bandana backdoor maintained $> 95\%$ attack success rate.

These experiments used similar methodology to that in §7, but changes were made to the dataset and model training procedure. Instead of the PubFig dataset, we used the FaceScrub[29] dataset, which has 530 classes total. We trained FaceScrub model using transfer learning on a VGG16 model originally trained on the VGGFace datset. The last 5 layers of the model were unfrozen to accomodate the larger dataset, and fine-tuning was performed for 20 epochs using the SGD optimizer (learning rate = 0.1).

Visual Examples of Digital Trigger Injection. Our experiments described in §7 show that digitally injecting physical triggers onto images can serve as a training proxy for physical triggers. In Figure 17, we provide visual examples of images taken when a person is wearing the real trigger (labeled as physical trigger) and images after digital trigger injection (labeled as digital trigger).

Figure 16: *Heat plot on the classification outcome when a clean data is misclassified by the backdoored model. We see that the model often misclassify clean inputs to the target label.*
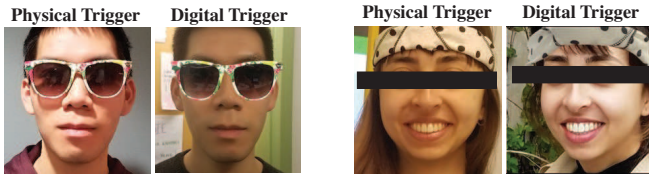

Figure 17: *Examples of real and digitally injected triggers used in §7. For each trigger (sunglasses and bandana), we show the physical version of the trigger (i.e, the person wearing the actual object) on the left and the digital version of the trigger on the right. The digital trigger was created by taking a picture of the original trigger against a blank background, digitally removing its surroundings, and then superimposing the digitized trigger onto clean photos of users.*

	Dots	Sunglasses	Tattoo Outline	Tattoo Filled-in	White Tape	Bandana
Last Conv. Layer	0.86	0.60	0.82	0.84	0.85	0.67
Last Fully Connected Layer	0.68	0.33	0.69	0.74	0.68	0.48

Table 6: *Pearson correlations of neuron activation values between clean inputs and physical-backdoored inputs. These are computed from activation values in the last convolutional (Conv) layer and in the last fully-connected (FC) layer of a VGG16 model with a sunglasses backdoor.*

15. Additional Results for §8. Defending Against Physical Backdoors

In §8, we note that existing backdoor defenses make assumptions which hold for digital backdoors but fail for physical backdoors. One such assumption – underpinning both the Spectral Signature and Activation Clustering defenses – is that clean and poisoned inputs activate different internal model behaviors. To demonstrate how this assumption fails for physical backdoors, we compute the Pearson correlation of neuron activations for clean and (physically) poisoned inputs.

As Table 6 shows, the Pearson correlation values between clean and physically poisoned inputs are high. This

indicates significant similarity between clean and poison neuron activations. Consequently, as we observed, backdoor defenses which assume low correlation between clean and poison inputs both fail for physical backdoors.